Journal of Alloys and Compounds 508 (2010) 206–211

Contents lists available at ScienceDirect

Journal of Alloys and Compounds

journal homepage: www.elsevier.com/locate/jallcom

Grain refining efficiency and microstructure of Al–Ti–C–RE master alloy

Hongliang Zhao*, Yong Song, Miao Li, Shaokang Guan

College of Materials Science & Engineering, Zhengzhou University, No. 97 Wenhua Road, Zhengzhou 450002, Henan, China

ARTICLE INFO

Article history:
Received 6 June 2010
Received in revised form 2 August 2010
Accepted 4 August 2010
Available online 19 August 2010

Keywords:
Al–Ti–C–RE
Microstructure
Grain refinement
Commercially pure aluminum

ABSTRACT

Al–Ti–C–RE master alloy has been successfully prepared by reaction of K_2TiF_6 salt, graphite powder and rare earth (RE) with Al. The microstructure of the alloy was characterized by optical microscopy, X-ray diffraction, scanning electron microscopy equipped with energy-dispersive spectrometry. The results show the microstructure of Al–Ti–C–RE alloy is composed of α-Al, lath-shaped $TiAl_3$, granular TiC, and blocky or rim $Ti_2Al_{20}Ce$. Compared with the Al–Ti–C master alloy, the addition of RE modifies the morphology of $TiAl_3$ phase, accelerates the formation of TiC. Al–Ti–C–RE alloy was used for grain refinement studies on commercial pure aluminum. An excellent grain refining performance was obtained when the addition level of Al–Ti–C–RE reaches to 0.5 wt%. The refinement mechanism of Al–Ti–C–RE has also been discussed.

1. Introduction

The addition of grain refiners is the most simple and effective method to improve comprehensive properties of aluminum products. Al–Ti–B grain refiner containing soluble $TiAl_3$ and insoluble TiB_2 particles is now widely used in aluminum industry. But there are still some problems for Al–Ti–B, such as agglomeration of the borides, blockage of filters, defects during subsequent forming operations and poisoning by certain elements like Zr, V and Cr [1–3]. Al–Ti–C master alloy, which contains dispersed TiC particles as the heterogeneous nuclei, was found to be free from problems mentioned above [4–7]. Unfortunately, poor wettability between graphite and liquid aluminum makes the fabrication of A1–Ti–C grain refiners difficult and prevents its application in industry.

The addition of rare earth elements in the preparation process of Al–Ti–B grain refiner can decrease the size of $TiAl_3$ and obtained dispersive distributed TiB_2 particles, by which the refining efficiency of Al–Ti–B was improved [8]. WU proposed that the wettability of liquid aluminum and graphite can be improved by adding small amount of Ce into molten aluminum [9]. The effect of La on the microstructure and refining efficiency of Al–Ti–C grain refiner was investigated, and the addition of La results in dispersive distribution of $TiAl_3$ and TiC particles in the matrix [10].

In this paper, a novel Al–5Ti–0.25C–2RE grain refiner is prepared by melt reaction method, and the microstructure of Al–5Ti–0.25C–2RE and its refining effect on commercially pure aluminum were investigated. The influences of RE addition on fabrication processing, morphology and distribution, and grain refining effect of Al–5Ti–0.25C–2RE were discussed.

2. Experimental details

Al–5Ti–0.25C–2RE was prepared by a liquid–solidification-reaction method. 99.7% commercial pure Al, commercial pure K_2TiF_6, graphite powder and Ce-rich mischmetal were used to prepare the Al–Ti–C–RE grain refiner. Firstly, commercial pure aluminum was melted in medium frequency furnace. The K_2TiF_6 which was preheated at 800 °C for 0.5–1 h and graphite powder which was preheated at 80 °C for 0.5–1 h were added to the superheated aluminum melt at 800–900 °C. About 4–7 min later, Ce-rich mischmetal (The composition of the Ce-rich mischmetal (wt%) was shown in Table 1) was added into the melt, which was stirred by a graphite stirrer. After 10 min, the temperature of the melt increased to 1200–1300 °C. Then the melt was kept for 10 min. After slag flux was eliminated, the melt was poured into a cast iron mold (25 mm in diameter and 100 mm in height) at 700–800 °C. Metallographic specimens of Al–5Ti–0.25C–2RE were taken from the center of each sample in the transverse section. The metallographic specimens were etched with 0.5 vol% hydrofluoric acid after mechanical polishing. Optical microscopy, scanning electron microscopy and energy-dispersive spectrometry were used to analyze their microstructures and components. X-ray diffraction was used to identify the phases of the specimen.

The refining tests were carried out by adding 0.1%, 0.3%, 0.5% and 0.7% of A1–Ti–C–RE grain refiners into 99.7% commercially pure A1 melts at 730 °C, then holding for 5 min, and pouring into a cast iron mold (20 mm in diameter and 100 mm in height). The samples were cut at a distance of 45 mm from the bottom, polished and etched by a reagent (60%HCl, 30%HNO_3, 5%HF and 5%H_2O), and the macrostructure of the samples were revealed.

3. Results and discussion

3.1. Microstructures of Al–5Ti–0.25C–2RE

From Fig. 1, it can be seen the Al–5Ti–0.25C–2RE alloy contains α-Al, $TiAl_3$, TiC and $Ti_2Al_{20}Ce$ phase. Discrete lath-like, blocky-like, enwrapped-like, particle-like and cluster-like phases in the Al

---

* Corresponding author. Tel.: +86 371 63887502; fax: +86 371 63886964.
E-mail address: zhlwkr@zzu.edu.cn (H. Zhao).

0925-8388/$ – see front matter © 2010 Elsevier B.V. All rights reserved.
doi:10.1016/j.jallcom.2010.08.047

Table 1
The composition of the Ce-rich mischmetal (wt%).

Element	Ce	La	Nb	Pr
Chemical composition	50.20%	26.67%	15.28%	5.37%

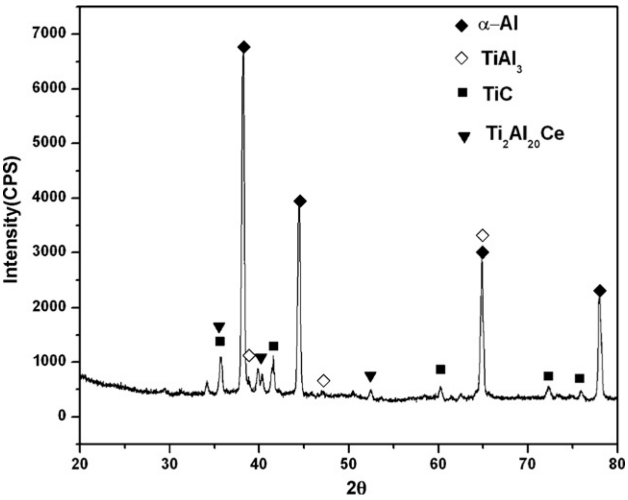

Fig. 1. XRD pattern of Al–5Ti–0.25C–2RE master alloy.

matrix can be observed in Fig. 2. Considering both the XRD (Fig. 1) and the EDS (Figs. 3 and 4), it can be presumed that the grayish regions are α-Al matrix, the discrete lath-like phase is $TiAl_3$, the cluster-like phase is TiC particles which agglomerate together according to the minimum energy principle, and the blocky-like and enwrapped-like phases are $Ti_2Al_{20}Ce$.

According to the EDS patterns in Fig. 3, it can be presumed that the enwrapped-like (Fig. 3b) and the blocky phase (Fig. 3d) are the same rare earth phase. The formation of $Ti_2Al_{20}Ce$ phases, which is due to the reaction between $TiAl_3$ and the dispersively distributed rare earth particles, can be explained as follows: the blocky $Ti_2Al_{20}Ce$ phase was formed by a complete reaction between the rare earth particles and small blocky $TiAl_3$ phase. Meanwhile, the rare earth particles also tend to adsorb onto the surface of the large plate-like $TiAl_3$, the enwrapped-like $Ti_2Al_{20}Ce$ phase was formed and grow up via incomplete peritectic reaction.

From Fig. 4, it can be seen that some near-spherical particles dispersed in the Al matrix, and some particles connect with each other to form cluster-like structures. The EDS spectrum of the fine particles shows the mole ratio of Ti to C of the phase is close to 1:1. Considering the XRD, the particles were identified as TiC phase. Due to the fineness of the TiC particles, the Al peak in the spectrum is possibly the contribution of the matrix Al.

Fig. 5a presents the optical micrograph of Al–5Ti–0.25C, which was prepared by the same method as Al–5Ti–0.25C–2RE but no rare earth elements were added. Comparing the optical micrograph of Al–5Ti–0.25C (Fig. 5a) and Al–5Ti–0.25C–2RE (Fig. 5b), which show that $TiAl_3$ is distributed in the a-A1 matrix in the form of needle-like for the A1–5Ti–0.25C sample, whereas $TiAl_3$ is lath-like which is much wider than needle-like for the A1–5Ti–0.25C–2RE sample. As seen in Fig. 5, measured by the Image Software, the TiC particles took 8.85% of the measurement area in master alloy without Ce, while the TiC particles took 29.62% of the measurement area in master alloy with Ce. The amount of TiC particles in Al–5Ti–0.25C–2RE is much more than that of A1–5Ti–0.25C. According to Ref. [11], grain refiner with needle-like $TiAl_3$ cannot obtain refinement as well as the one with lath-like $TiAl_3$. Better refining efficiency was obtained with the increasing amount of TiC particles, which act as the heterogeneous nuclei for α-Al.

3.2. Grain refinement of commercial pure aluminum by Al–5Ti–0.25C–2RE

Fig. 6 shows macrographs of as-cast commercially pure aluminum grain refined with 0.1%, 0.3%, 0.5%, 0.7% addition level of Al–5Ti–0.25C-2RE and 0.5% addition level of Al–5Ti–0.25C. As Fig. 6a shows, the commercial pure aluminum without grain refiner exhibits coarse columnar grains. When 0.1% Al–5Ti–0.25C–2RE was added, the commercial pure aluminum exhibits a mixture of coarse columnar grains and equiaxed grains, and the average grain size was also decreased. Increased the addition level of grain refiner up to 0.3%, fine equiaxed grains were obtained instead of the columnar grains, and the average grain size was significantly decreased. Fig. 7 shows the relationship of grain size and the addition level of grain refiner. When 0.5% grain refiner is added, the average grain size reaches the minimum. But further increase the addition level of grain refiner shows no significant improvement in grain refining efficiency.

Fig. 6f and c shows macrographs of as-cast commercial pure aluminum after adding 0.5 wt% A1–5Ti–0.25C and A1–5Ti–0.25C–2RE, respectively. It can be obviously seen that the grain size of aluminum refined by A1–5Ti–0.25C–2RE (110 μm in average) is much lower than that of A1–5Ti–0.25C (190 μm in average). The specimen (Fig. 6f) refined by A1–5Ti–0.25C exhibits a mixture of coarse columnar grains and equiaxed grains, however the specimen (Fig. 6c) refined by A1–5Ti–0.25C–2RE exhibits fine equiaxed grains instead of the columnar grains.

Table 2 shows the tensile strength and elongation of the commercial pure aluminum refined by adding Al–5Ti–0.25C and Al–5Ti–0.25C–2RE. It indicates that the mechanical properties of

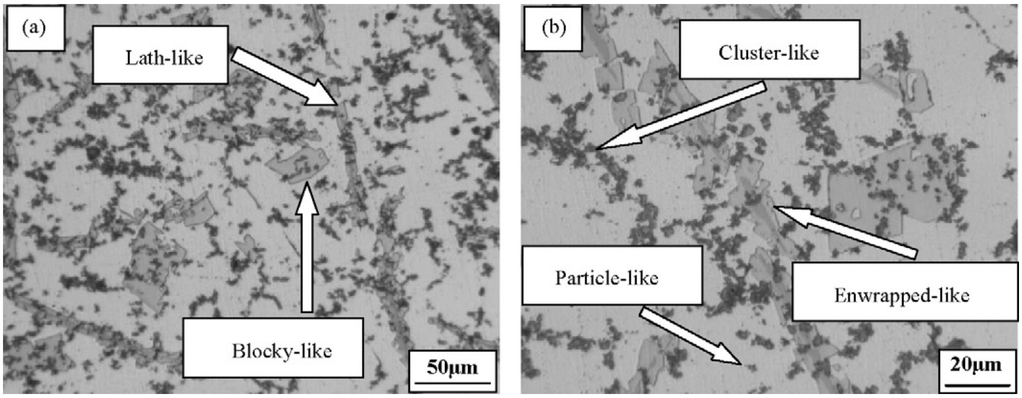

Fig. 2. Optical micrograph of Al–5Ti–0.25C–2RE master alloy.

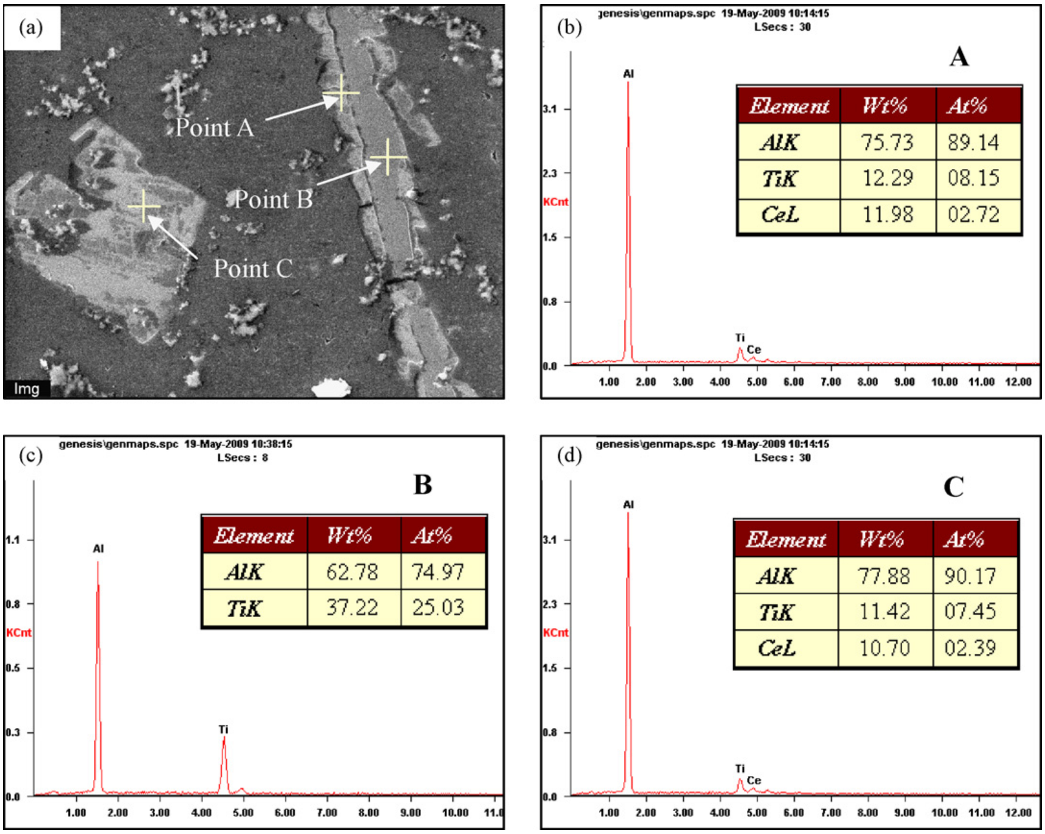

A

Element	Wt%	At%
AlK	75.73	89.14
TiK	12.29	08.15
CeL	11.98	02.72

B

Element	Wt%	At%
AlK	62.78	74.97
TiK	37.22	25.03

C

Element	Wt%	At%
AlK	77.88	90.17
TiK	11.42	07.45
CeL	10.70	02.39

Fig. 3. (a) SEM micrograph of Al–5Ti–0.25C–2RE alloy, (b) EDS pattern of point A, (c) EDS pattern of point B, and (d) EDS pattern of point C.

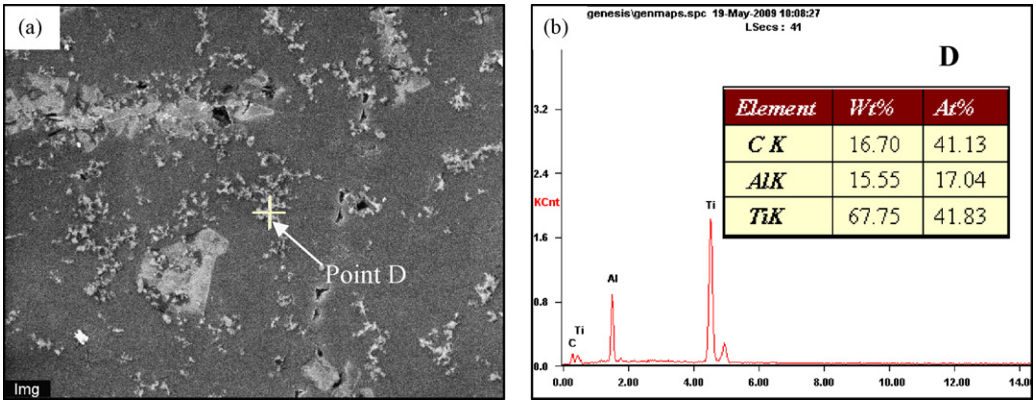

D

Element	Wt%	At%
C K	16.70	41.13
AlK	15.55	17.04
TiK	67.75	41.83

Fig. 4. (a) SEM micrograph of TiC in Al–5Ti–0.25C–2RE alloy and (b) EDS pattern of point D.

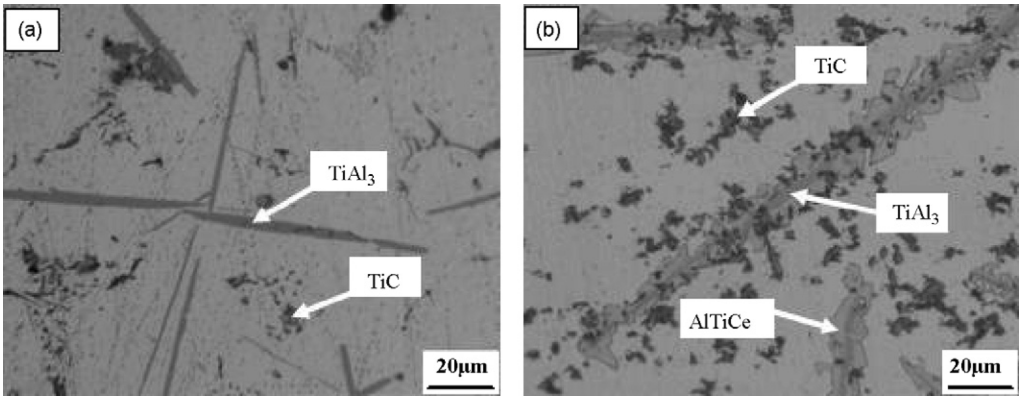

Fig. 5. (a) Optical micrograph of Al–5Ti–0.25C and (b) optical micrograph of Al–5Ti–0.25C–2RE.

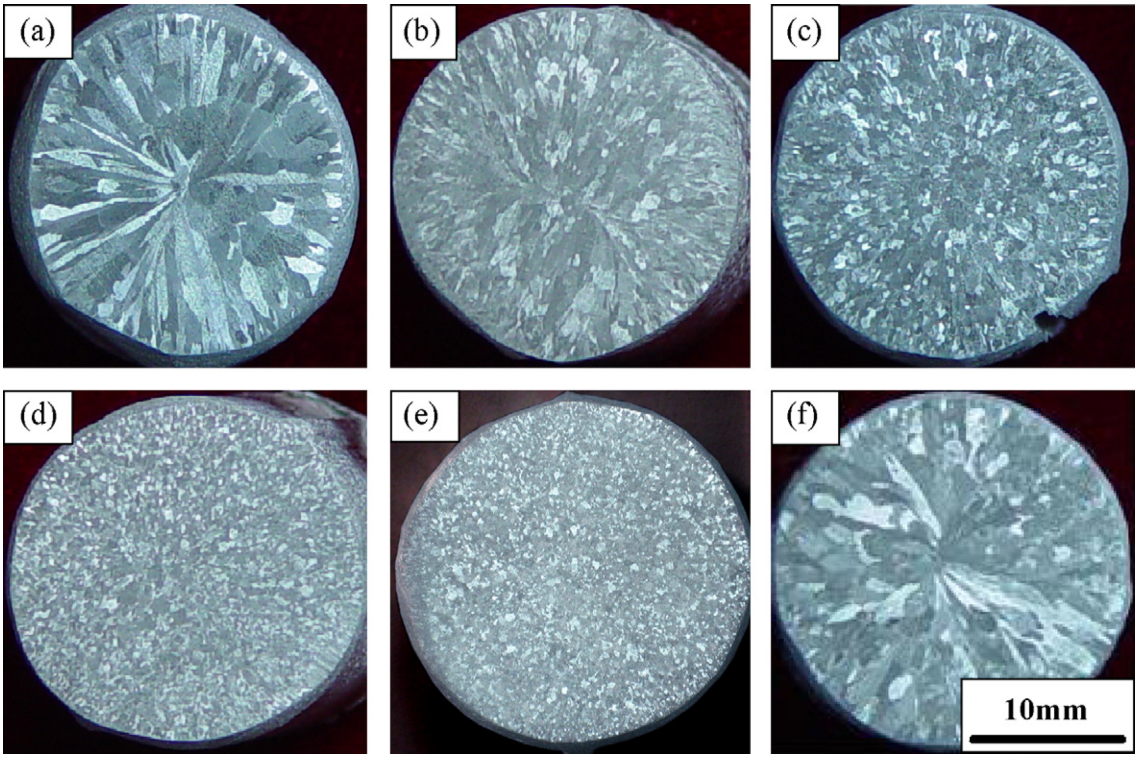

Fig. 6. Macrograph of commercial pure aluminum refined using A1–5Ti–0.25C–2RE or Al–5Ti–0.25C. (a) Pure aluminum; (b) 0.1% A1–5Ti–0.25C–2RE; (c) 0.3% A1–5Ti–0.25C–2RE; (d) 0.5% A1–5Ti–0.25C–2RE; (e) 0.7% A1–5Ti–0.25C–2RE; (f) 0.5% Al–5Ti–0.25C.

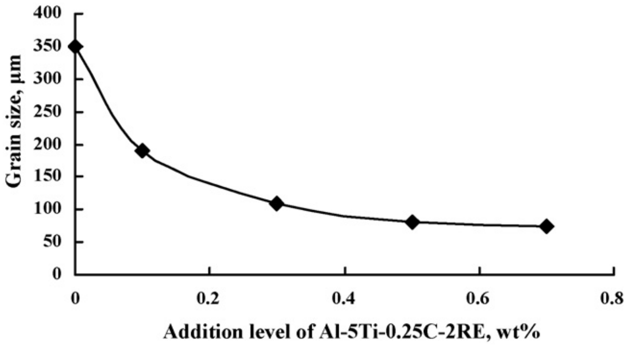

Fig. 7. The relationship of grain size and the addition level of grain refiner.

commercial pure aluminum increased with the decreasing of the average grain size. The tensile strength and elongation of the commercial pure aluminum refined by 0.5 wt% Al–5Ti–0.25C increased by 5.6% and 7.7%, respectively, compared with the initial commercial pure aluminum. When 0.5 wt% Al–5Ti–0.25C–2RE was added, the tensile strength and elongation of the commercially pure aluminum increased by 10.4% and 19.2% respectively, compared to the initial commercially pure aluminum.

It is very clear from Fig. 8 that, the alloy shows fast grain refinement response with 0.5 wt% addition of Al–Ti–C–RE master alloy and the grain structure becomes finer within 5 min and remains the same even after 120 min of holding. The results clearly show that 0.5 wt% Al–Ti–C–RE can refine the commercial pure aluminum at all holding time without fading.

Table 2
Tensile strength and elongation of commercially pure aluminum.

	Pure aluminum	Pure aluminum + 0.5%Al–5Ti–0.25C	Pure aluminum + 0.5%Al–5Ti–0.25C–2RE
Tensile strength σ_b (MPa)	59.93	63.28	66.19
Elongation δ (%)	43.33	46.67	51.67

3.3. Discussion

(1) Effect of RE in Al–Ti–C preparing process

To improve the wettability between graphite and liquid aluminum is a key problem for preparing A1–Ti–C grain refiner. Normally, the solubility of graphite in liquid aluminum is limited, some methods have been used for graphite to wet liquid aluminum such as preheating the graphite, elevating the temperature of aluminum melt after the graphite is added, and strongly mechanical stirring. Besides the treatments mentioned above, the addition of mischmetal can reduce the surface energy of graphite, lowers the wetting angle, and accelerate the rate of reaction between graphite powder and aluminum melt, which are all because of the absorption of RE on the surface of graphite particles. It can be seen from the micrographs (Fig. 5) that the amount of TiC particles in Al–5Ti–0.25C–2RE increased greatly compared with that in Al–5Ti–0.25C, which proved that the addition of mischmetal accelerated the absorption of graphite.

Compared the micrographs of Al–5Ti–0.25C with Al–5Ti–0.25C–2RE (Fig. 5), it can be seen that the $TiA1_3$ phase distributed in A1–5Ti–0.25C as needle-like, but transformed to lath-like with the addition of mischmetal. This may be attributed to the $Ti_2Al_{20}Ce$ phase, which enwrapped around $TiA1_3$ and suppressed the growth of $TiA1_3$. The mischmetal can not only accelerate the formation of TiC particles, but also prevent TiC particles from changing into Al_4C_3 by agglomerated around TiC particles, and increase the spreading coefficient of TiC, by which TiC particles can hardly form cluster and sediment.

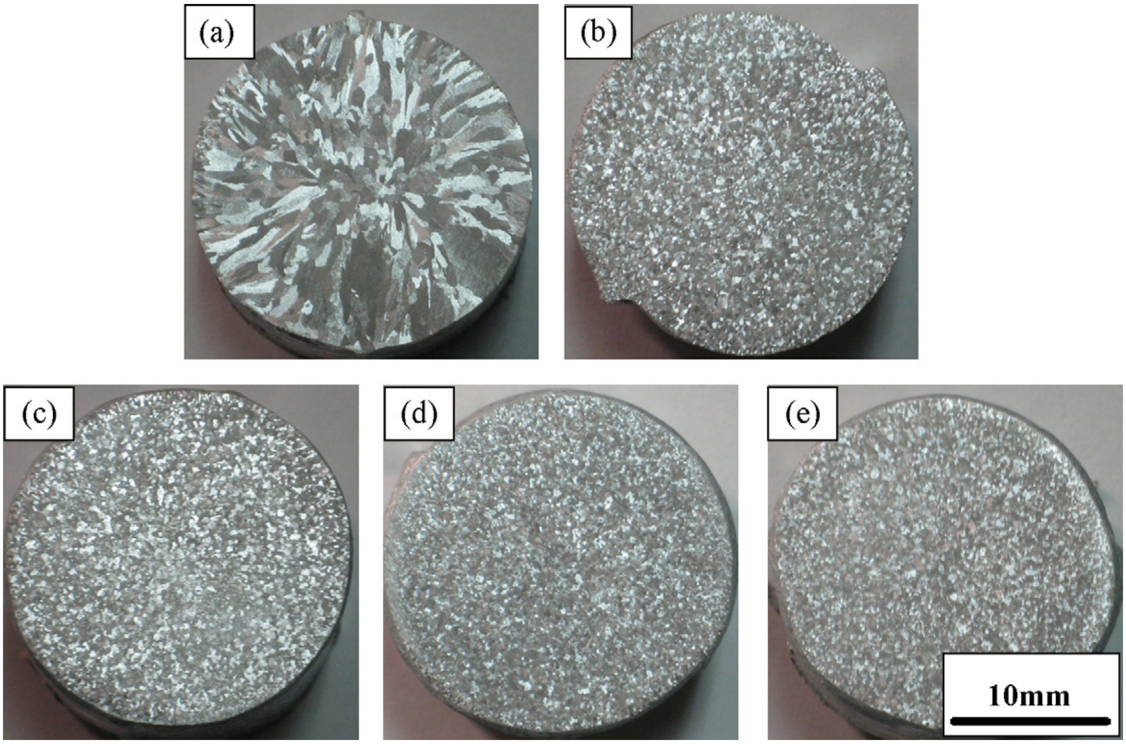

Fig. 8. Macrographs of commercially pure aluminum refined using 0.5 wt% A1–5Ti–0.25C–2RE. (a) 0 min; (b) 15 min; (c) 30 min; (d) 60 min; (e) 120 min.

(2) Grain refinement mechanism of Al–Ti–C–RE

In the Al–Ti–C–RE refiner, TiC particles, which surrounded by Ti atoms layer, act as efficient substrates for nucleation of aluminum. Ti atoms layer act as a powerful protective layer to avoid the formation of Al_4C_3 phase during processing. When the refiner was added to Al melt, a thin layer of $TiAl_3$ was formed by the extra Ti atoms with Al atoms. Furthermore, α-Al was formed and grew via peritectic reaction between the $TiAl_3$ layer and Al atoms around in the solidification processing. Comparing the Al–Ti–C–RE refiner with Al–Ti–C refiner, Ti atom was not only existed in lath-like $TiAl_3$ phase but also detected in the blocky and rim $Ti_2Al_{20}Ce$ phase.

DTA (differential thermal analysis) was used in order to analyze the role of $Ti_2Al_{20}Ce$ in refining process and the heating rate during the DTA analysis was 10 °C per minute. The DTA curve (Fig. 9) shows three endothermic peaks located at 630 °C, 670 °C and 910 °C. Because of the higher melting temperature of $TiAl_3$ and TiC phases they have, the endothermic peak located at 630 °C is due to the decomposition of $Ti_2Al_{20}Ce$ phase. The strong endothermic effect at 670 °C is corresponding to the melting of the Al matrix, and the weak endothermic at 910 °C is due to the decomposition of $TiAl_3$ phase.

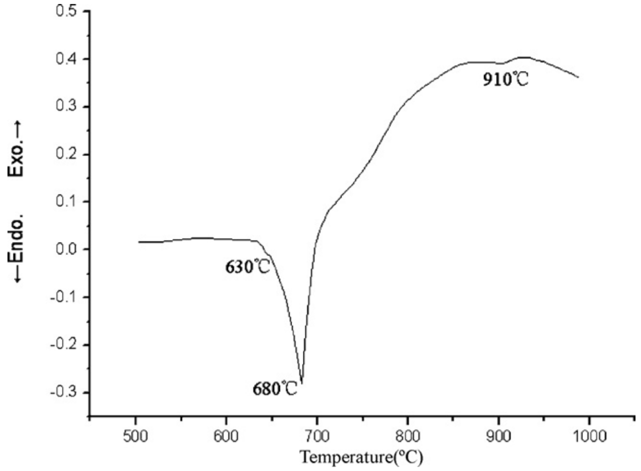

Fig. 9. DTA curve of Al–5Ti–0.25C–2RE master alloy.

On the basis of DTA examination, the melting of $Ti_2Al_{20}Ce$ was earlier than that of $TiAl_3$ with the temperature rising. An excessive amount of Ti atoms may aggregate to the TiC surface with different morphology of $Ti_2Al_{20}Ce$ phase release Ti atoms, which leads TiC to be efficient heterogeneous nuclei of α-Al and makes the refiner show fast grain refinement response. Meanwhile, the melting of $Ti_2Al_{20}Ce$ can ensure the existence of $TiAl_3$ in a long holding time, which will reduce the refinement fading on longer holding time.

It has been found that the $Ti_2Al_{20}Ce$ phase as intermetallic compound is unstable, and dissolved with temperature rising in the refining process [12]. The released rare earth atoms combined with other dissociative atoms form an intermetallic compound with high melting point, which can act as heterogeneous nucleus for α-Al [13]. It has also been found that the atomic radius of rare earth elements is larger than that of aluminum atom and rare earth is kind of surfactant, so there will be an aggregation of rare earth elements on the grain boundary of α-Al, which can decrease the surface activity of α-Al, and consequently suppresses the growth of α-Al. The low growing speed of crystals and much more crystal nuclei created by rare earth elements will decrease the grain sizes. It has also been found [14] that adding some rare earth into aluminum alloy can refine the casting grains. The rare earth elements may also cause constitutional supercooling because of the solute redistribution in front of solid/liquid interface, which enhanced the kinetics of α-Al nucleation.

4. Conclusions

Al–5Ti–0.25C–2RE master alloy which was prepared by a melt reaction method consists of phases for α-Al, lath-like $TiAl_3$, particle-like or cluster-like TiC, and blocky-like and enwrapped-like $Ti_2Al_{20}Ce$. And it shows better grain refining efficiency than that of A1–5Ti–0.25C. The addition of mischmetal accelerates the formation of TiC, reduces the agglomeration tendency of TiC particles, modified the morphology of $TiAl_3$ phase, and resulted in excellent grain refining efficiency.

References

[1] Y. Birol, J. Alloys Compd. 430 (2007) 179–187.
[2] A.A. Rao, B.S. Murty, M. Chakraborty, Mater. Sci. Technol. 13 (1997) 769.
[3] M. Johnsson, Z. Metallkd. 85 (1994) 786.
[4] Y.L. Li, H.K. Feng, F.R. Cao, Y.B. Chen, L.Y. Gong, Mater. Sci. Eng. A 487 (2008) 518–523.
[5] X.F. Liu, Z.Q. Wang, Z.G. Zhang, X.F. Bian, Mater. Sci. Eng. A 332 (2002) 70–74.
[6] G.S. Kumar, B.S. Murty, M. Chakraborty, J. Alloys Compd. 396 (2005) 143–150.
[7] A. Banerji, W. Reif, Metall. Trans. A 17 (1986) 2127.
[8] Y.J. Chen, Q.Y. Xu, T.Y. Huang, J. Tsinghua University 47 (2007) 618–622 (in Chinese).
[9] S.Q. Wu, Y.P. Liu, Met. Sci. Technol. 5 (1986) 92–98 (in Chinese).
[10] C.X. Xu, L.P. Liang, B.F. Lu, et al., J. Rare Earths 24 (2006) 596–601.
[11] C.X. Xu, J.S. Zhang, Mater. Sci. Technol. 9 (2001) 166–168 (in Chinese).
[12] G. Fu, W. Chen, K. Qian, J. Rare Earth 21 (2003) 547–575.
[13] Y.F. Lan, P. Guo, J.J. Zhang, Foundry Technol. 26 (2005) 774–775 (in Chinese).
[14] X.R. Zuo, L.X. Li, Z.G. Zhong, Foundry Technol. 28 (2007) 57–59 (in Chinese).